

# Vibration mitigation of composite laminated satellite solar panels using distributed piezoelectric patches

M.A. Foda\* and K.A. Alsaif

*Mechanical Engineering Department College of engineering, King Saud University  
P.O. Box 800, Riyadh 11421, Saudi Arabia*

*(Received September 23, 2011, Revised May 28, 2012, Accepted June 21, 2012)*

**Abstract.** Satellites with flexible lightweight solar panels are sensitive to vibration that is caused by internal actuators such as reaction or momentum wheels which are used to control the attitude of the satellite. Any infinitesimal amount of unbalance in the reaction wheels rotors will impose a harmonic excitation which may interact with the solar panels structure. Therefore, quenching the solar panel's vibration is of a practical importance. In the present work, the panels are modeled as laminated composite beam using first-order shear deformation laminated plate theory which accounts for rotational inertia as well as shear deformation effects. The vibration suppression is achieved by bonding patches of piezoelectric material with suitable dimensions at selected locations along the panel. These patches are actuated by driving control voltages. The governing equations for the system are formulated and the dynamic Green's functions are used to present an exact yet simple solution for the problem. A guide lines is proposed for determining the values of the driving voltage in order to suppress the induced vibration.

**Keywords:** vibration mitigation; piezoelectric patches; Green's function; composite Timoshenko beam

---

## 1. Introduction

The fiber-reinforced composite materials replaced conventional materials in many applications in aeronautics and astronautics industries. They are widely used in fabrication of many components such as flaps, stabilizers, rudders, solar panels, rotary blades,...etc. The attractiveness of composites lies in their flexibility in design and their mechanical properties; such as weight, strength, stiffness, corrosion resistance, and fatigue life. The laminate mechanical properties can be altered by changing the stacking sequence, fibre lay-up and thickness of each ply which leads to optimization in a design process. Composite structures integrated with piezoelectric elements as actuators and sensors are widely used in aerospace industries. Piezoelectric actuators have proved to be effective, inexpensive, reliable, and non-intrusive control devices for structural vibration control and suppression. The early investigation of piezoelectric materials to control vibration was carried out by Olson (1965). Now they are integrated in various structural components that are used in a wide range of engineering applications (Tzou 1993, Bank *et al.* 1996, Preumont 2002). During the past few decades, a significant amount of literature reporting studies on the analysis of smart structures with surface or embedded piezoelectric sensors and actuators has been devoted to structural vibration control (Srinivasan 2001,

---

\*Corresponding author, Professor, E-mail: [mfoda@ksu.edu.sa](mailto:mfoda@ksu.edu.sa)

Ma and Ghasen 2004). An active vibration damper for a cantilever beam was designed using a distributed-parameter actuator (a piezoelectric polymer) and distributed-parameter control theory by Bailey and Hubbard (1995). Hagood and Chung (1990) established an analytical model for general structures with piezoelectric materials using Hamilton principle and demonstrated the applications of the general models using a cantilevered beam. Garcia *et al.* (1995) developed an active control method to suppress vibrations of flexible ribbed antenna structures using piezoceramic components as both sensor and actuator simultaneously. Kim *et al.* (1995) applied optimal control theory to reduce the vibration of a flexible space structure produced by the reaction wheel. A systematic method for selecting an optimal set of locations and the minimal number of piezoelectric actuators and sensors was applied by using an effectiveness index based on the combined degree of controllability and observability of each structural mode. Kayacik *et al.* (2008) used integral approach to control the damped free vibration of Euler Bernoulli cantilever beam with bonded piezoelectric patches as sensors and actuators. Honda *et al.* (2011) discussed a multidisciplinary design optimization technique of a smart composite plate with piezoelectric actuators. They used finite elements, a simple genetic algorithm and  $H_2$  control method to optimize both the lay-up configurations and the actuator placements simultaneously. More recently, Kedziora and Muc (2012) investigated the electromechanical couplings and control of piezoelectric laminated cylindrical shells and rectangular plates using finite elements and an evolutionary algorithm. Their aim is to find the optimal ply orientation angles of layers and actuators' configurations to control the deflections and natural frequencies.

In the current paper, a methodology is developed to quench the transverse vibration of satellite solar panels using piezoelectric patches with suitable dimensions. These patches are bonded to the panels at selected locations by using strong adhesive material and are driven by electrical voltages. The panels are modeled as composite laminated beam using first-order shear deformation laminated plate theory which accounts for rotational inertia as well as shear deformation effects. Incorporation of the shear effects in the analysis of laminated composite is important due to the lower transverse shear modulus compared to the extensional modulus. A key feature of the present work is that the problem is formulated in terms of the Green's functions. This method is exact and straightforward. It is computationally efficient and numerically accurate and this can be used as an aid to validate other approximate methods like modal superposition or finite element. The boundary conditions are embedded in the Green's function; consequently it is not necessary to solve the free vibration problem in order to obtain the eigenvalues and the corresponding eigenfunctions, which are required for modal superposition solution. Design guide is provided to determine the values of the driving voltages required to quench the vibration of the panels. Numerical simulations, using MATLAB; is performed to verify the utility of the proposed method.

Following this introduction, Section 2 describes the formulation of the problem. The solution procedure is given in Section 3. Design guide to quench vibration is given in section 4. Numerical simulations and results are shown in Section 5. The paper closes with summary and some conclusions in Section 6.

## 2. Analytical formulation

### 2.1 Panel model

Fig. 1 shows a simple physical schematic of micro-satellite with flexible solar panels subjected to harmonic excitations due to the unbalance of the reactions wheels. Rather than modeling this system

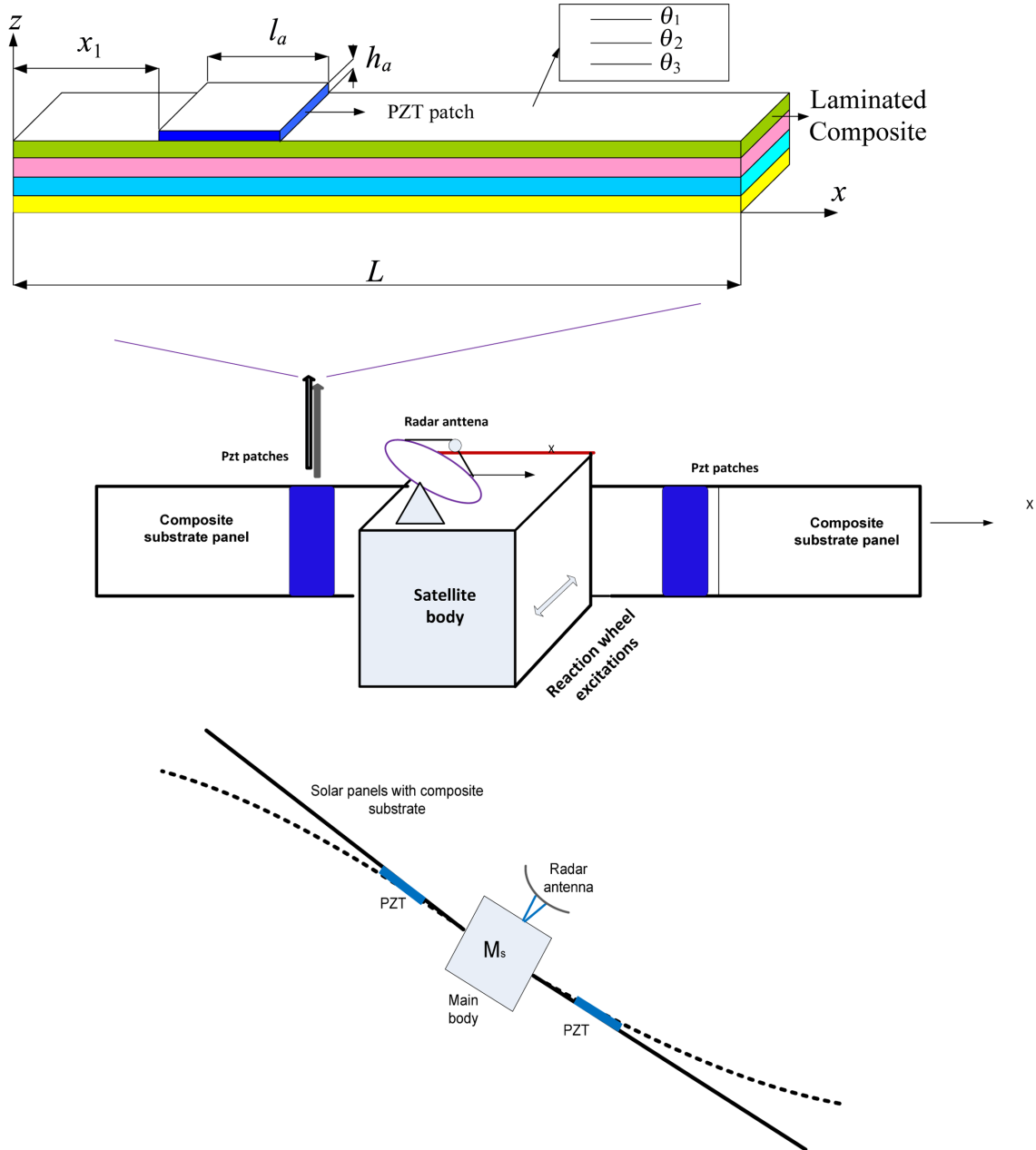


Fig. 1 Schematic of a satellite with flexible composite solar panels with bonded piezoelectric patches subjected to a harmonic excitation

as two identical beams of length  $L/2$ , it is rather advantageous to consider a free-free beam of length  $L$  with attached satellite mass at its mid-point. This viewpoint is reasonable since the satellite body's dimensions are much less than beam length. Fig. 2 represents a simple model for the actual physical system. It consists of a uniform elastic laminated composite beam of rectangular cross section of height  $2h_b$  and width  $b$ . This beam is presumed to be made of perfectly  $N$  orthotropic bonded

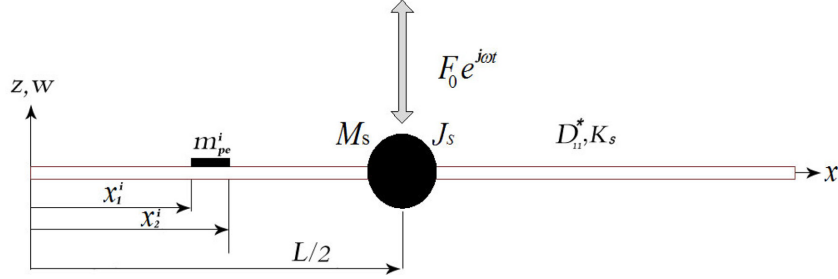


Fig. 2 Schematic simplified model

symmetric laminae such that no lamina can slip relative to another. The mass of the satellite is represented by  $M_s$  attached at  $x=L/2$  associated with mass moment of inertia  $J_s$ . There are  $N_p$  piezoelectric patches (wafers) acted as actuators,  $x_1^i$  and  $x_2^i$  are the coordinates of the left and the right edges of the  $i$ th patch; respectively, and each has thickness  $h_a$ . The external force  $f_{ext}(x,t)$  is assumed to be given by the real part of the following expression

$$f_{ext}(x,t) = F_0 e^{j\omega t} \delta(x-x_f) \quad (1)$$

where  $\omega$  is the excitation frequency,  $\delta(\cdot)$  is the spatial Dirac delta singularity function,  $F_0$  is the amplitude of the applied force, and  $j = \sqrt{-1}$  is the imaginary unit.

## 2.2 Rigidities of laminated panel

The constitutive relations (see Appendix A) are based on the first order shear deformation laminated plate theory (see Jones 1975). In this theory it is assumed that the two first Kirchhoff hypotheses hold: the transverse normal to the mid-surface before the deformation remains straight after deformation and do not experience elongation. In addition, Mindlin assumption: the transverse normal does not remain perpendicular to the mid-surface after deformation is invoked. With the last assumption, the gross transverse shear deformation is included in the kinematic assumptions of the classical laminated plate theory as an improvement.

Upon assuming that  $M_{yy} = M_{xy} = Q_y = \phi_y = 0$  in Eq. (A7), we obtain

$$M_{xx} = D_{11}^* \frac{\partial \phi_x}{\partial x}, \quad Q_x = k' A_{55}^* \left( \frac{\partial w}{\partial x} + \phi_x \right) \quad (2a,b)$$

where

$$D_{11}^* = D_{11} + (2D_{12}D_{16}D_{26} - D_{12}^2D_{66} - D_{16}^2D_{22}) / (D_{22}D_{66} - D_{26}^2)$$

$$A_{55}^* = (A_{55} - A_{45}^2/A_{44}) \quad (3)$$

The shear correction factor  $k'$  depends on the lamina properties and stacking sequence, and also on the width to depth ratio in a rectangular cross section. It is introduced to correct for the discrepancy between the constant distributed transverse shear stress predicted by the first-order theory and the actual distribution obtained from the three-dimensional elasticity theory. In this work,  $k' = 5/6$  was used, as in a rectangular section of a homogeneous Timoshenko beam because the differences between this shear-

correction factor and that for the corresponding composite beam are not significant as demonstrated in (Vinson and Sierakowski 1986, Madabhusi and Davalos 1996).

It is apparent that the flexural rigidity and the transverse shear rigidity of the composite beam are  $D_{11}^*$  and  $k'A_{55}^*$ ; respectively compared to  $EI$  and  $k'GA$  of the Timoshenko homogenous beam.

### 2.3 Governing equation

Neglecting beam axial inertia, the expression of the total kinetic energy of the system can be written as

$$T = \frac{1}{2} \int_0^L \left\{ I_0 \left( \frac{\partial w(x,t)}{\partial t} \right)^2 + I_0 \left( \frac{\partial \psi(x,t)}{\partial t} \right)^2 + M_s \left( \frac{\partial w(x,t)}{\partial t} \right)^2 \delta(x-L/2) + J_s \left( \frac{\partial \psi(x,t)}{\partial t} \right)^2 \delta(x-L/2) \right\} dx \quad (4)$$

Where  $w = w_0$ ,  $\psi = \phi_x$ ,  $\delta(\cdot)$  is the Dirac delta singularity function. The mass moment of inertias are given by

$$(I_0, I_2) = b \sum_{i=1}^{k=N} \int_{-h_b}^{h_b} \rho^{(k)}(1, z^2) dz \quad (5)$$

The potential energy can be written as

$$U = \frac{1}{2} \int_0^L \left[ D_{11}^* \left( \frac{\partial \psi(x,t)}{\partial x} \right)^2 + k'A_{55}^* \left( \frac{\partial w(x,t)}{\partial x} + \psi(x,t) \right)^2 \right] dx \quad (6)$$

The equations of motion can now be derived by applying Hamilton's principle

$$\int_{t_1}^{t_2} \delta(T - U + W_{nc}) dt = 0 \quad (7)$$

where  $W_{nc}$  denotes the work done by the external forces (non-conservative forces) and can be expressed as

$$W_{nc} = \int_0^L [q(x,t)w(x,t) + M_{pe}(x,t)\psi(x,t)] dx \quad (8)$$

where  $q(x,t)$  and  $M_{pe}(x,t)$  are generalized force and moment; respectively which can be expressed as.

$$q(x,t) = F_0 e^{j\omega t} \delta(x-x_f) + \sum_{i=1}^{i=N_p} f_{pe}^i(x,t) \quad (9a)$$

$$M_{pe}(x,t) = \sum_{i=1}^{i=N_p} \bar{M}_{pe}^i(t) [H(x-x_1^i) - H(x-x_2^i)] \quad (9b)$$

Where  $f_{pe}^i(x,t)$  is the transverse inertia of the  $i$ th piezoelectric patch,  $x_1^i$  and  $x_2^i$  are the left and right edge coordinates of  $i$ th piezoelectric patch; respectively.  $H(\cdot)$  is the Heaviside step function and  $\bar{M}_{pe}^i(t)$  is the actuation moment amplitude produced by the  $i$ th piezoelectric patch. If the length of the patch is very small compared to the length of the beam, the transverse inertia force of the  $i$ th patch can be

considered as concentrated force acting at its midpoint. Therefore  $f_{pe}^i(x, t) = m_{pe}^i \frac{\partial^2 w}{\partial t^2} \delta(x - x_m^i)$  where  $m_{pe}^i$  and  $x_m^i = (x_1^i + x_2^i)/2$  are the mass and the midpoint of the  $i$ th patch respectively. In Chen and Shen (1999) early work, the inertial effects of the piezoelectric elements are ignored because they are thin and of lightweights compared to the beam system.

Substituting the expressions for  $T$ ,  $U$  and  $W_{nc}$  in the standard form of Hamilton's principle, Eq. (7), and then performing the usual variation, the following governing equations are derived

$$D_{11}^* \frac{\partial^2 \psi}{\partial x^2} - k'A_{55}^* \left( \frac{\partial w}{\partial x} + \psi \right) - I_2 \frac{\partial^2 \psi}{\partial t^2} - J_s \frac{\partial^2 \psi}{\partial t^2} \delta(x - L/2) + \frac{\partial M_{pe}(x, t)}{\partial x} = 0 \quad (10)$$

$$I_0 \frac{\partial^2 w}{\partial t^2} - k'A_{55}^* \left( \frac{\partial^2 w}{\partial x^2} + \frac{\partial \psi}{\partial x} \right) + M_s \frac{\partial^2 w}{\partial t^2} \delta(x - L/2) = q(x, t) \quad (11)$$

The associated boundary conditions are

$$\frac{\partial \psi}{\partial x} = 0, \frac{\partial w}{\partial x} + \psi = 0, \text{ at } x = 0 \text{ and } x = L \quad (12)$$

### 2.3 Constitutive equations for piezoelectric patches

The linear constitutive equation relating the coupling between the elastic and electric fields for a piezoelectric material is expressed by the direct and inverse piezoelectric relations. Using the IEEE (1988) on piezoelectricity standard; (see Moulson and Herbert 1990) and assuming plane stress, the one dimensional electromechanical constitutive equation is written as

$$\begin{Bmatrix} \sigma_1 \\ D_3 \end{Bmatrix} = \begin{bmatrix} E_{pe} & -d_{31}E_{pe} \\ d_{31}E_{pe} & \beta_3^T - d_{31}^2 E_{pe} \end{bmatrix} \begin{Bmatrix} \varepsilon_1 \\ E_3 \end{Bmatrix} \quad (13)$$

where  $D_3$  denotes the electric displacement (charge/unit area) along the beam transverse direction ( $z$ -direction),  $E_3$  represents the applied electric field density (Volt/unit length) along the transverse direction,  $\varepsilon_1$  and  $\sigma_1$  represents the mechanical strain and stress; respectively, in the axial direction ( $x$ -direction),  $\beta_3^T$  denotes the permittivity of the piezoelectric material,  $d_{31}$  denotes the piezoelectric strain constant and  $E_{pe}$  is the Young's modulus of the piezoelectric material. The last three constants are generally obtained from the piezoelectric manufacturer.

The relation between the electric voltage and the electric field is

$$E = V(t)/h_a \quad (14)$$

where  $V(t)$  is the voltage applied in thickness direction in the case of an actuator and it is the induced voltage in the case of a sensor.

It is assumed that the piezoelectric patch is long in  $x$  and in  $y$  directions compared to thickness in the  $z$ -direction and it is assumed to be isotropic with constant properties along its length. In addition, the piezoelectric patch is perfectly bonded to the panel and the strain in the  $y$ -direction is neglected since the problem is formulated as a one-dimensional beam problem. When a voltage is applied across the piezoelectric element, a strain  $\varepsilon_{pe}$  is induced in the  $x$ -direction

$$\varepsilon_{pe} = d_{31}V/h_a \quad (15)$$

Where  $V$  is the applied voltage in the direction of polarization and  $d_{31}$  is the piezoelectric material strain constant. For a perfect bonding, the beam will both bend and stretch leading to asymmetric linear stress distribution. Following Gibbs and Fuller (1999), applying both moment equilibrium about the center of the beam and the force equilibrium over the beam cross section we obtain the moment amplitude induced beneath the  $i$ th patch as given by (Foda *et al.* 2010)

$$\bar{M}_{pe}^i = c^i D_{11}^* \frac{d_{31}^i V^i(t)}{h_a^i} \quad (16)$$

where

$$c^i = 12E_{pe}^i h_a^i [I_6 (h_a^i / 2 + h_b) - I_5] / [12I_4 I_6 + I_6 E_{pe}^i h_a^i (4h_a^i h_a^i + 12h_a^i h_b + 12h_b^2) + 12I_4 E_{pe}^i h_a^i - 12I_5^2 - 12I_5 E_{pe}^i h_a^i (h_a^i + 2h_b) + (E_{pe}^i h_a^i h_a^i)^2], \quad (17)$$

and

$$(I_4, I_5, I_6) = \sum_{k=1}^{k=N} \int_{z_k}^{z_{k+1}} \tilde{Q}_{11}^{(k)}(z^2, z, 1) dz, \quad \tilde{Q}_{11}^{(k)} = \left( \bar{Q}_{11} - \frac{\bar{Q}_{12} \bar{Q}_{12}}{\bar{Q}_{22}} \right) \quad (18)$$

If the width of the beam is  $b$  and that of the piezoelectric element is  $b_{pe}^i$ , the previous equations still hold but  $E_{pe}^i$  should be replaced by  $E_{pe}^i b_{pe}^i / b$ . A final added note is concerned with the asymptotic value of  $c^i$  for small values of  $h_a^i / h_b$ . Without much analysis one can prove that for  $h_a^i / h_b \ll 1$ ,  $c^i \sim 1/h_b$ .

### 3. Solution procedure

The field equations; Eqs. (10) and (11) are coupled and it is advantageous for the subsequent analysis to transform them into a single equation. Hence we introduce an auxiliary variable  $y(x, t)$  such that (Li 2008).

$$w = y - \frac{D_{11}^* \partial^2 y}{k' A_{55}^* \partial x^2} + \frac{I_2 \partial^2 y}{k' A_{55}^* \partial t^2}, \quad \psi = -\frac{\partial y}{\partial x} \quad (19a, b)$$

Differentiating Eq. (10) *w.r.t*  $x$ , substituting for  $\partial \psi / \partial x$  from Eq. (19(b)) and utilizing Eq. (11) and Eq. (19(a)) we obtain a single fourth order partial differential equation for the variable  $y(x, t)$

$$\begin{aligned} D_{11}^* \frac{\partial^4 y}{\partial x^4} + I_0 \frac{\partial^2 y}{\partial t^2} - \left( I_2 + \frac{I_0 D_{11}^*}{K_s} \right) \frac{\partial^4 y}{\partial t^2 \partial x^2} + \frac{I_0 I_2}{K_s} \frac{\partial^4 y}{\partial t^4} = q \\ - M_s \left( \frac{\partial^2 y}{\partial t^2} - \frac{D_{11}^*}{K_s} \frac{\partial^4 y}{\partial t^2 \partial x^2} + \frac{I_2}{K_s} \frac{\partial^4 y}{\partial t^4} \right) \delta(x - L/2) + J_s \frac{\partial^4 y}{\partial t^2 \partial x^2} \delta(x - L/2) \\ + \frac{\partial^2 M_{pe}(x, t)}{\partial x^2} - \sum_{i=1}^{i=N_p} m_{pe}^i \left( \frac{\partial^2 y}{\partial t^2} - \frac{D_{11}^*}{K_s} \frac{\partial^4 y}{\partial t^2 \partial x^2} + \frac{I_2}{K_s} \frac{\partial^4 y}{\partial t^4} \right) \delta(x - x_m^i) \end{aligned} \quad (20)$$

Where  $K_s = k' A_{55}^*$  is the shear rigidity.

Using Eqs. (19(a) and (b)), the corresponding boundary conditions given by Eq. (12) become

$$\frac{\partial^2 y}{\partial x^2} = 0, \quad \frac{\partial^3 y}{\partial x^3} - \frac{I_2}{D_{11}^*} \frac{\partial^3 y}{\partial t^2 \partial x} = 0, \quad \text{at } x = 0, x = L \quad (21)$$

We now seek a solution of Eq. (20) subjected to the associated boundary conditions, Eq. (20). Since the excitation is a sinusoidal function with frequency  $\omega$ , the sought solution takes the form

$$y(x, t) = Y(x)e^{j\omega t}, \quad V^i(t) = V_0^i e^{j\omega t} \quad (22)$$

The substitution of Eq. (22) into Eq. (20), and making use of Eqs. (9) and (16), the time dependence is cancelled out and reduces it to

$$\begin{aligned} & \frac{d^4 Y}{dx^4} + \frac{\omega^2}{D_{11}^*} \left( I_2 + \frac{I_0 D_{11}^*}{K_s} \right) \frac{d^2 Y}{dx^2} - \frac{I_0 \omega^2}{D_{11}^*} \left( 1 - \frac{I_2 \omega^2}{K_s} \right) Y = \frac{F_0}{D_{11}^*} \delta(x - x_f) \\ & + \left[ \frac{M_s \omega^2}{D_{11}^*} \left( 1 - \frac{I_2 \omega^2}{K_s} \right) Y - \omega^2 \left( \frac{M_s}{K_s} + \frac{J_s}{D_{11}^*} \right) \frac{d^2 Y}{dx^2} \right] \delta(x - L/2) \\ & + \sum_{i=1}^{i=N_p} c^i \frac{d_{31}^i V_0^i}{h_a^i} [\delta'(x - x_1^i) - \delta'(x - x_2^i)] + \\ & + \frac{\omega^2}{D_{11}^*} \sum_{i=1}^{i=N_p} m_{pe}^i \left[ \left( 1 - \frac{I_2 \omega^2}{K_s} \right) Y - \frac{D_{11}^*}{K_s} \frac{d^2 Y}{dx^2} \right] \delta(x - x_m^i) \end{aligned} \quad (23)$$

In the work to be followed it is highly advantageous to work with dimensionless quantities so that the numerical results are applicable for large combinations of system parameters and the analysis becomes general. Hence, the following non-dimensional variables and coefficients are introduced

$$\begin{aligned} \hat{x} &= x/L, \quad \hat{\omega} = \omega/\omega_0, \quad \hat{Y} = Y/Y_0, \quad \hat{c}^i = Lc^i, \quad \hat{h}_a^i = h_a^i/L \\ \hat{M}_s &= M_s/I_0 L, \quad \hat{J}_s = J_s/I_0 L^2, \quad \hat{V}_0^i = V_0^i d_{31}^i/Y_0, \quad \hat{m}_{pe}^i = m_{pe}^i/I_0 L \end{aligned} \quad (24)$$

Where

$$Y_0 = F_0 L^3 / D_{11}^*, \quad \omega_0 = \sqrt{D_{11}^* / I_0 L^4} \quad (25)$$

Therefore the non-dimensional form of Eq. (23) is

$$\begin{aligned} & \hat{Y}'''' - \frac{\hat{\omega}^2}{I_0 L^2} \left( I_2 + \frac{I_0 D_{11}^*}{K_s} \right) \hat{Y}'' - \hat{\omega}^2 \left( 1 - \frac{I_2 D_{11}^* \hat{\omega}^2}{K_s I_0 L^4} \right) \hat{Y} = \hat{\delta}(\hat{x} - \hat{x}_f) \\ & + \left[ \hat{M}_s \hat{\omega}^2 \left( 1 - \frac{I_2 D_{11}^* \hat{\omega}^2}{K_s I_0 L^4} \right) \hat{Y} - \hat{\omega}^2 \left( \hat{M}_s \frac{D_{11}^*}{K_s L^2} + \hat{J}_s \right) \hat{Y}'' \right] \hat{\delta}(\hat{x} - 0.5) \\ & + \sum_{i=1}^{i=N_p} \hat{M}_{pe}^i [\hat{\delta}'(\hat{x} - \hat{x}_1^i) - \hat{\delta}'(\hat{x} - \hat{x}_2^i)] + \hat{\omega}^2 \sum_{i=1}^{i=N_p} \hat{m}_{pe}^i \left[ \left( 1 - \frac{I_2 D_{11}^* \hat{\omega}^2}{K_s I_0 L^4} \right) \hat{Y} - \frac{D_{11}^*}{K_s L^2} \hat{Y}'' \right] \hat{\delta}(\hat{x} - \hat{x}_m^i) \end{aligned} \quad (26a)$$

Where

$$\hat{M}_{pe}^i = \frac{\hat{c}^i \hat{V}_0^i}{\hat{h}_a^i} \quad (26b)$$

The prime denotes derivative with respect to  $\hat{x}$  and  $\hat{\delta}(\hat{x}) = L\delta(x)$ .

The associated non-dimensional boundary conditions are

$$\frac{d^2\hat{Y}}{d\hat{x}^2} = 0, \quad \frac{d^3\hat{Y}}{d\hat{x}^3} + \frac{I_2\hat{\omega}^2}{D_{11}^*} \frac{d\hat{Y}}{d\hat{x}} = 0, \quad \text{at } \hat{x} = 0, \hat{x} = 1 \quad (26c)$$

Therefore, the non-dimensional governing equation is in the form

$$\hat{Y}'''' - \lambda\hat{Y}'' - \beta\hat{Y} = Q(x) \quad (27)$$

where

$$\begin{aligned} Q(\hat{x}) = & \hat{\delta}(\hat{x} - \hat{x}_f) + [\hat{M}_s\beta\hat{Y} - \hat{\omega}^2(\hat{M}_s\frac{D_{11}^*}{K_sL^2} + \hat{J}_s)\hat{Y}'']\hat{\delta}(\hat{x} - 0.5) \\ & + \sum_{i=1}^{i=N_p} \hat{c}^i \frac{d_{31}^i\hat{V}_0^i}{\hat{h}_a^i} [\hat{\delta}'(\hat{x} - \hat{x}_1^i) - \hat{\delta}'(\hat{x} - \hat{x}_2^i)] + \sum_{i=1}^{i=N_p} \hat{m}_{pe}^i [\beta\hat{Y} - \frac{\hat{\omega}^2 D_{11}^*}{K_s L^2} \hat{Y}''] \hat{\delta}(\hat{x} - \hat{x}_m^i) \end{aligned} \quad (28)$$

and

$$\lambda = \hat{\omega}^2 \left( \frac{I_2}{I_0 L^2} + \frac{D_{11}^*}{K_s L^2} \right), \quad \beta = \hat{\omega}^2 \left( 1 - \frac{I_2 D_{11}^* \hat{\omega}^2}{K_s I_0 L^4} \right) \quad (29)$$

The dynamic Green's function is utilized to find the solution for Eq. (27). Hence if  $\hat{G}(\hat{x}, \hat{u})$  is the nondimensional dynamic Green function for the stated problem, then the solution of Eq. (27) takes the form

$$\hat{Y}(\hat{x}) = \int_0^1 \hat{G}(\hat{x}, \hat{u}) Q(\hat{u}) d\hat{u} \quad (30)$$

Performing the integration using the properties of the Dirac delta function, one obtains the following exact form solution

$$\begin{aligned} \hat{Y}(\hat{x}) = & \hat{G}(\hat{x}, \hat{x}_f) + [\hat{M}_s\beta\hat{Y}(0.5) - \hat{\omega}^2(\hat{M}_s\frac{D_{11}^*}{K_sL^2} + \hat{J}_s)\hat{Y}''(0.5)]\hat{G}(\hat{x}, 0.5) \\ & + \sum_{i=1}^{i=N} \hat{M}_{pe}^i [\hat{G}_{\hat{u}}(\hat{x}, \hat{x}_2^i) - \hat{G}_{\hat{u}}(\hat{x}, \hat{x}_1^i)] + \sum_{i=1}^{i=N} \hat{m}_{pe}^i [\beta\hat{Y}(\hat{x}_m^i) - \frac{\hat{\omega}^2 D_{11}^*}{K_s L^2} \hat{Y}''(\hat{x}_m^i)] \hat{G}(\hat{x}, \hat{x}_m^i) \end{aligned} \quad (31)$$

The second derivative of Eq. (31) with respect to  $\hat{x}$  is

$$\begin{aligned} \hat{Y}''(\hat{x}) = & \hat{G}_{\hat{x}\hat{x}}(\hat{x}, \hat{x}_f) + [\hat{M}_s\beta\hat{Y}(0.5) - \hat{\omega}^2(\hat{M}_s\frac{D_{11}^*}{K_sL^2} + \hat{J}_s)\hat{Y}''(0.5)]\hat{G}_{\hat{x}\hat{x}}(\hat{x}, 0.5) \\ & + \sum_{i=1}^{i=N} \hat{M}_{pe}^i [\hat{G}_{\hat{u}\hat{x}\hat{x}}(\hat{x}, \hat{x}_2^i) - \hat{G}_{\hat{u}\hat{x}\hat{x}}(\hat{x}, \hat{x}_1^i)] + \sum_{i=1}^{i=N} \hat{m}_{pe}^i [\beta\hat{Y}(\hat{x}_m^i) - \frac{\hat{\omega}^2 D_{11}^*}{K_s L^2} \hat{Y}''(\hat{x}_m^i)] \hat{G}(\hat{x}, \hat{x}_m^i) \end{aligned} \quad (32)$$

where  $\hat{G}_{\hat{u}} = \frac{\partial \hat{G}(\hat{x}, \hat{u})}{\partial \hat{u}}$ ,  $\hat{G}_{\hat{x}\hat{x}} = \frac{\partial^2 \hat{G}(\hat{x}, \hat{u})}{\partial \hat{x}^2}$ , and  $\hat{G}_{\hat{u}\hat{x}\hat{x}} = \frac{\partial^3 \hat{G}(\hat{x}, \hat{u})}{\partial \hat{u} \partial \hat{x}^2}$

The Green's function is the solution of the differential equation

$$\hat{G}''''(\hat{x}, \hat{u}) - \lambda \hat{G}''(\hat{x}, \hat{u}) - \beta \hat{G}(\hat{x}, \hat{u}) = \hat{\delta}(\hat{x} - \hat{u}) \quad (33)$$

which is given by

$$\hat{G}(\hat{x}, \hat{u}) = A \cosh p_1 \hat{x} + B \sinh p_1 \hat{x} + C \cos p_2 \hat{x} + D \sin p_2 \hat{x} + \hat{\phi}(\hat{x}, \hat{u}) \quad (34)$$

where

$$\hat{\phi}(\hat{x}, \hat{u}) = \frac{H(\hat{x} - \hat{u})}{p_1^2 + p_2^2} \left( \frac{\sinh p_1(\hat{x} - \hat{u})}{p_1} - \frac{\sin p_2(\hat{x} - \hat{u})}{p_2} \right) \quad (35)$$

and

$$p_1 = \sqrt{\frac{\sqrt{4\beta + \lambda^2} + \lambda}{2}}, \quad p_2 = \sqrt{\frac{\sqrt{4\beta + \lambda^2} - \lambda}{2}} \quad (36a,b)$$

The constants  $A$ ,  $B$ ,  $C$  and  $D$  are obtained from satisfying the boundary conditions at the ends as given by Eq. (26(b)). The Green's function can be very useful when dealing with linear systems, see Roach (1981). One can derive the Green's function by using the conventional approach (Bergman and Hyatt 2003) or by using the Laplace transformation (Abo-Hilal 2003).

To this end, one evaluates  $\hat{Y}(\hat{x})$  and  $\hat{Y}''(\hat{x})$  from Eqs. (31) and (32); respectively, at  $\hat{x} = 0.5$  and at  $\hat{x}_m^i$  for  $i=1$  to  $N_p$ . This gives  $2N_p+2$  algebraic equations in the unknowns

$$\hat{Y}(0.5), \hat{Y}(\hat{x}_m^1), \dots, \hat{Y}(\hat{x}_m^{N_p}), \hat{Y}''(0.5), \hat{Y}''(\hat{x}_m^1), \dots, \hat{Y}''(\hat{x}_m^{N_p})$$

These equations can be solved then the results are substituted back into Eqs. (31) and (32). The panel transverse deflection is obtained from the nondimensional form Eq. (19(a)); specifically

$$\hat{W}(\hat{x}) = \left( 1 - \frac{I_2 D_{11}^* \hat{\omega}^2}{K_s I_0 L^4} \right) \hat{Y}(\hat{x}) - \frac{D_{11}^*}{K_s L^2} \hat{Y}''(\hat{x}) \quad (37)$$

Before closing this section we should mention that the formulation presented is applicable to any composite beam structure with boundary conditions other than free-free ends. This is because the boundary conditions are impeded in the derived Green's function of a specific beam. The Green's function  $G(x, u)$  for a system describes the displacement of the system at point  $x$  which is due to a unit force applied at point  $u$ . It depends only upon differential equation being examined and the boundary conditions which are imposed. Physically, it is the frequency response function of the system.

#### 4. Vibration mitigation

The vibration mitigation along the entire panel can be achieved near resonance conditions. In this case the transverse vibration of the panel is a simple spatial flexural waveform that can be cancelled by a single opposing wave that will be created by the PZT patches. The best location of the PZT patch is such that its mid-point coincides with the peak or through of the flexural wave, since at any of these positions the magnitude of the flexural displacement is a maximum (Foda *et al.* 2010). Therefore one selects the parameters  $\hat{x}_f$ ,  $\hat{l}_a^i$ ,  $\hat{h}_a^i$  and  $\hat{x}_m$  then find the applied voltage  $\hat{V}_0^i$  that are required for suppressing the vibration of the panel. This can be achieved by enforcing the amplitude

at location of a peak or a trough,  $\hat{x}_p$ , of the flexural wave to be zero. As indicated by Eq. (37), the sufficient conditions that the transverse deflection  $\hat{W}(\hat{x})$  at any point,  $\hat{x}$ , is zero is that  $\hat{Y}(\hat{x}) = \hat{Y}'''(\hat{x}) = 0$ . Based on the foregoing discussion, the following design guideline is suggested;

1. Given  $\hat{\omega}$ ,  $\hat{x}_f$  and the desired peak location  $\hat{x}_p$ , choose the patch parameters  $\hat{x}_m$ ,  $\hat{l}_a^i$ , and  $\hat{h}_a^i$ .
2. Solve for the actuation moments  $\hat{M}_{pe}^i$  and the deflection  $\hat{Y}(0.5), Y(\hat{x}_m^1), \dots, \hat{Y}(\hat{x}_m^{N_p}), \hat{Y}'''(0.5), \hat{Y}'''(\hat{x}_m^1), \dots, \hat{Y}'''(\hat{x}_m^{N_p})$
3. Compute the driving control voltage  $\hat{V}_0^i$  from Eq. (26(b))
4. Finally, at any point  $\hat{x}$  on the panel,  $\hat{Y}(\hat{x})$  and  $\hat{Y}'''(\hat{x})$  are calculated using Eqs. (31) and (32), then the deflection  $\hat{W}(\hat{x})$  can be calculated by the aid of Eq. (37).

## 5. Results of numerical simulation

In this section, several numerical examples are conducted to illustrate the utility and applicability of the proposed approach for quenching the vibration during the harmonic excitations of composite laminated satellite panels. The laminate layers are made of equal thickness and with lamination scheme  $(0^\circ/90^\circ/0^\circ)$ , which is a symmetric cross-ply laminate. The composite layers are made of TA5/3501-6 graphite-epoxy with the following properties (Abramovich and Livshits 1993).

$E_1 = 145$  GPa,  $E_2 = 9.6$  GPa,  $G_{31} = 4.1$  GPa,  $\rho = 1540$  kg/m<sup>3</sup>,  $\nu_{12} = 0.3$ . The PZT (G1195) has a piezoelectric constant  $d_{31} = -1.66 \times 10^{-12}$  (mV<sup>-1</sup>), Young modulus  $E_{pe} = 6.3 \times 10^{10}$  N/m<sup>2</sup>, density  $\rho_{pe} = 7650$  kg/m<sup>3</sup>. In all figures, the solid curve corresponds to the deformed shape of the system with bonded PZT patches while the dashed line represents the deformed shape of the bare panel (without bonded patches). The panel with bonded patches is called loaded panel. The height of the  $i$ th patch  $\hat{h}_a^i = 0.01 \hat{h}$  and its length  $\hat{l}_a^i = 0.08$ , the satellite mass  $\hat{M}_s = 10$  and its mass moment of inertia  $\hat{J}_s = 0$ , and location of the excitation  $\hat{x}_f = 0.5$ ; unless otherwise stated.

Fig. 3 presents the dynamic responses of bare and loaded panel when it is excited by a force with frequency  $\hat{\omega} = 118$  which is close to the fifth natural frequency of the bare panel ( $\hat{\omega}_5 = 120.7362$ ).

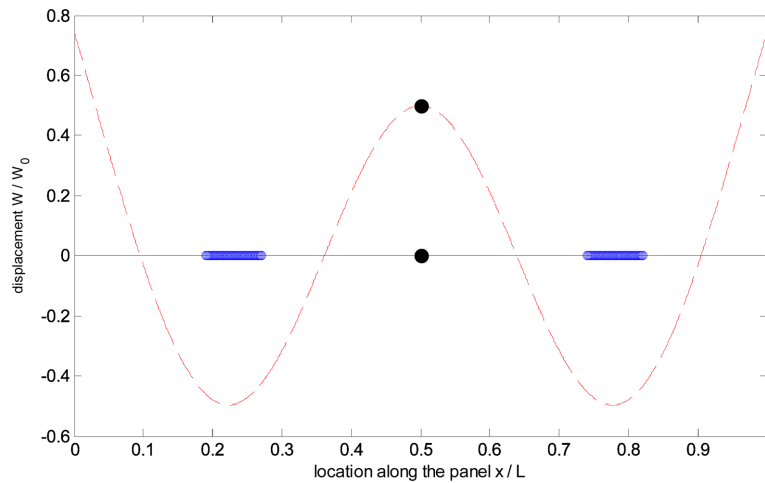


Fig. 3 The steady state deflection responses of loaded and unloaded panel when  $\hat{\omega} = 118$ ,  $x_m^1 = 0.23$ ,  $\hat{x}_m^2 = 0.77$ ,  $\hat{V}_0^1 = 0.00304 \times 10^{-6}$ ,  $\hat{V}_0^2 = -0.90249 \times 10^{-6}$ ; —, loaded; - - - - -, bare; ● mass  $M_s$

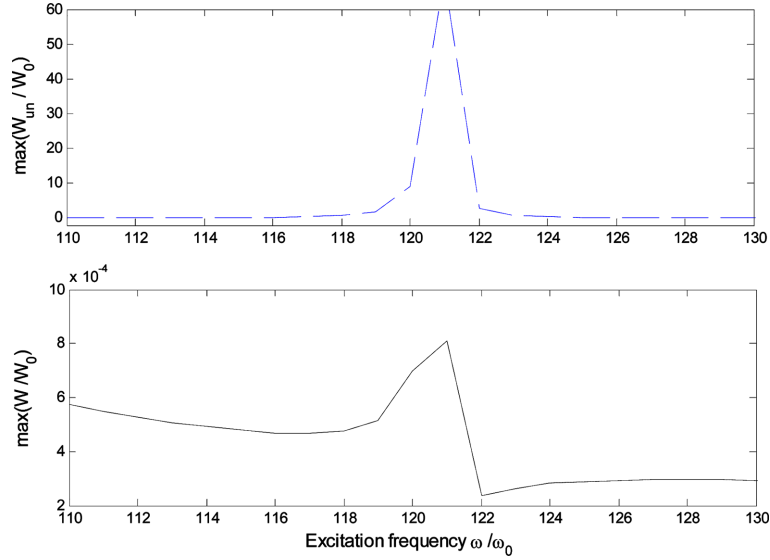


Fig. 4 Variation of the maximum deflection amplitudes versus the excitation frequency when  $\hat{V}_0^1 = 0.00304 \times 10^{-6}$ ,  $\hat{V}_0^2 = -0.90249 \times 10^{-6}$

Two PZT patches driven by control voltages are used to suppress the vibration of the system. The mid-point of the first patch is at  $\hat{x}_m^1 = 0.23$  while the mid-point of the second patch is at  $\hat{x}_m^2 = 0.78$ . The control voltages that required to make the system motionless are found to be  $\hat{V}_0^1 = 0.00304 \times 10^{-6}$  and  $\hat{V}_0^2 = -0.90245 \times 10^{-6}$ . Physically, the moments of the bonded PZT patches creates anti-waves that cancel the original flexural wave created by the external force. This effect is similar to that of the dynamic vibration absorber, which is used to quench the vibration of the harmonically excited single degree of freedom system. Comparable phenomenon is encountered in active noise cancellation by introducing an annihilating signal (anti-sound), Lueg (1936).

Fig. 4 compares the maximum deflection amplitudes of the controlled and un-controlled system as a function of the excitation frequency  $\hat{\omega}$  for the system given in Fig. 3. The PZT patches mid-point locations and the value of the control voltages are held fixed. As revealed by Fig. 3, near resonance the vibration of the controlled panel is substantially suppressed. In Fig. 5, the control voltages are plotted as a function of the mid-point locations of the PZT patches  $\hat{x}_m^i$  for the same system given in Fig. 3. Considerable information can be drawn from Fig. 5 in terms of stability, optimality and robustness. Here optimality is based on the minimum control voltages requirement. It may be observed that there are optimal mid-point locations of the PZT patches where the control voltages are minimal. The required control voltages when the patch mid-point location coincides with the nodes (the deflection amplitude  $\hat{W}(\hat{x}) = 0$ ) of the uncontrolled panel is relatively large. The flatness of the control force over the panel span is a direct indication of robustness.

Fig. 6 shows the same system as in Fig. 3 but the excitation frequency  $\hat{\omega} = 245$ . Two similar piezoelectric patches are bonded to the panel. The midpoint of the first patch is chosen to be at  $\hat{x}_m^1 = 0.15$  while the mid-point of the second is at  $\hat{x}_m^2 = 0.85$ . The driving control voltages are found to be  $\hat{V}_0^1 = -0.0016 \times 10^{-6}$  and  $\hat{V}_0^2 = 82.067 \times 10^{-6}$ . In Fig. 7, the excitation frequency  $\hat{\omega} = 14.4$  which is close to the first natural frequency of the bare panel ( $\hat{\omega}_1 = 14.4699$ ). Two similar piezoelectric are

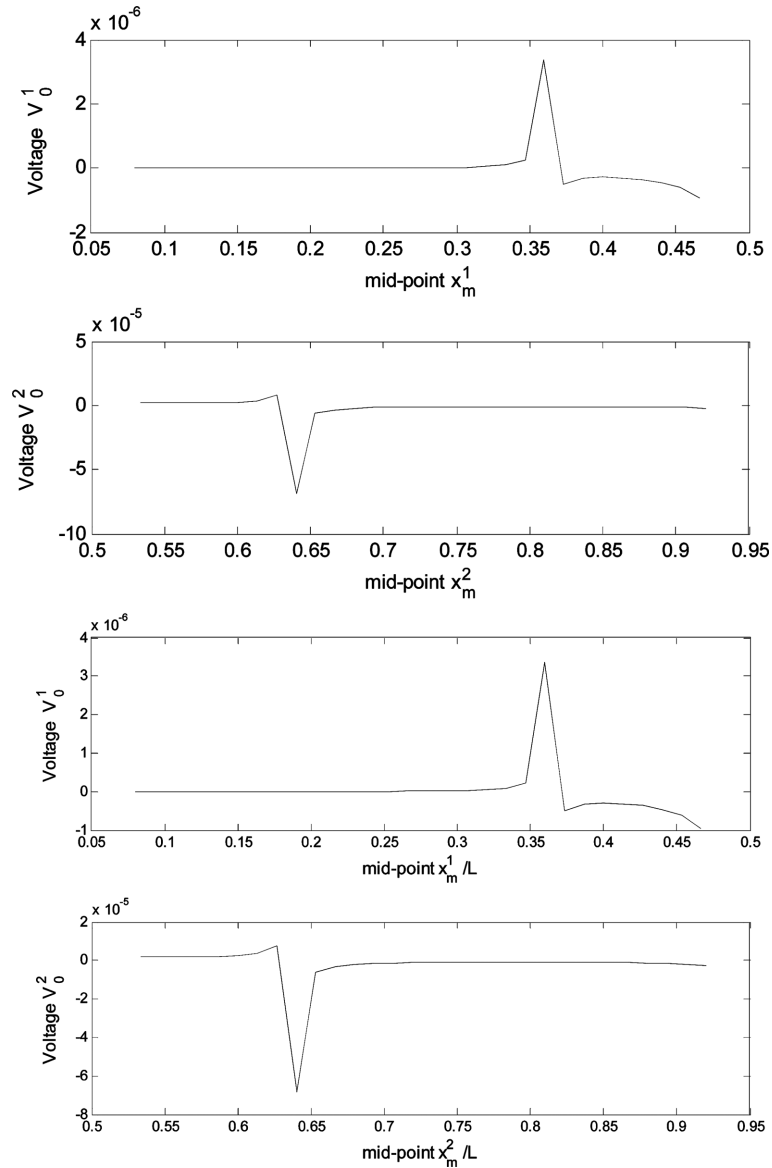


Fig. 5 Variation of the required control voltages versus locations of mid-points of the patches when  $\hat{\omega} = 118$

bonded to the panel. The mid-point of the first patch is chosen to be at  $\hat{x}_m^1=0.1$  while of the second patch is at  $\hat{x}_m^2=0.9$ . The driving control voltages are found to be  $\hat{V}_0^1=-0.0032 \times 10^{-5}$  and  $\hat{V}_0^2=0.3364 \times 10^{-5}$ . In Fig. 8, the location of the excitation force  $\hat{x}_f=0.45$  and the excitation frequency  $\hat{\omega}=61.5$ . The midpoint of the first patch is chosen to be at  $\hat{x}_m^1=0.3$  while the midpoint of the second is at  $\hat{x}_m^2=0.7$ . The driving control voltages are found to be  $\hat{V}_0^1=0.0256 \times 10^{-6}$  and  $\hat{V}_0^2=-0.5144 \times 10^{-6}$ . The last example depicts the dynamic responses of bare and loaded panel for which  $\hat{J}_s=0.5$  when it is excited by a force with frequency  $\hat{\omega}=70$ . Two similar piezoelectric patches are bonded to the panel. The midpoint of the first patch is chosen to be at  $\hat{x}_m^1=0.3$  while the mid-

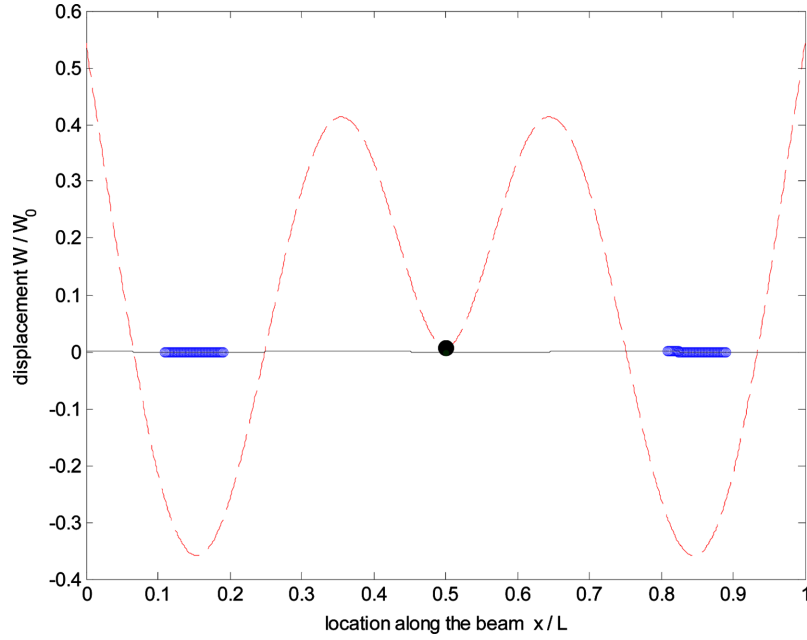


Fig. 6 The steady state deflection responses of loaded and unloaded panel when  $\hat{\omega} = 245$ ,  $\hat{x}_m^1 = 0.15$ ,  $\hat{x}_m^2 = 0.85$ ,  $\hat{V}_0^1 = -0.0016 \times 10^{-6}$ ,  $\hat{V}_0^2 = 82.067 \times 10^{-6}$ ; —, loaded; -----, bare; ●,  $M_s$

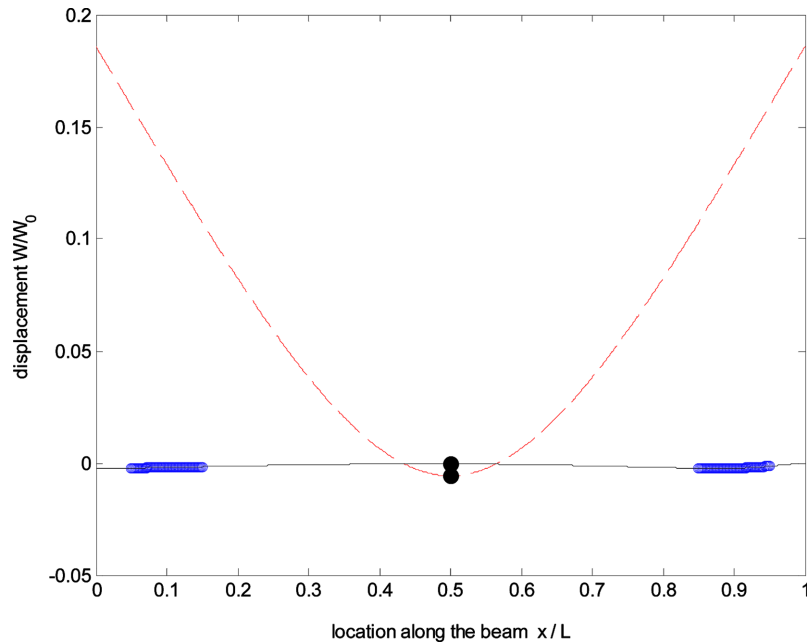


Fig. 7 The steady state deflection responses of loaded and unloaded panel when  $\hat{\omega} = 14.4$ ,  $\hat{x}_m^1 = 0.1$ ,  $\hat{x}_m^2 = 0.9$ ,  $\hat{l}_a^1 = 0.1$ ,  $\hat{l}_a^2 = 0.1$ ,  $\hat{V}_0^1 = -0.0032 \times 10^{-5}$ ,  $\hat{V}_0^2 = 0.3364 \times 10^{-5}$ ; —, loaded; -----, bare; ●, mass  $M_s$

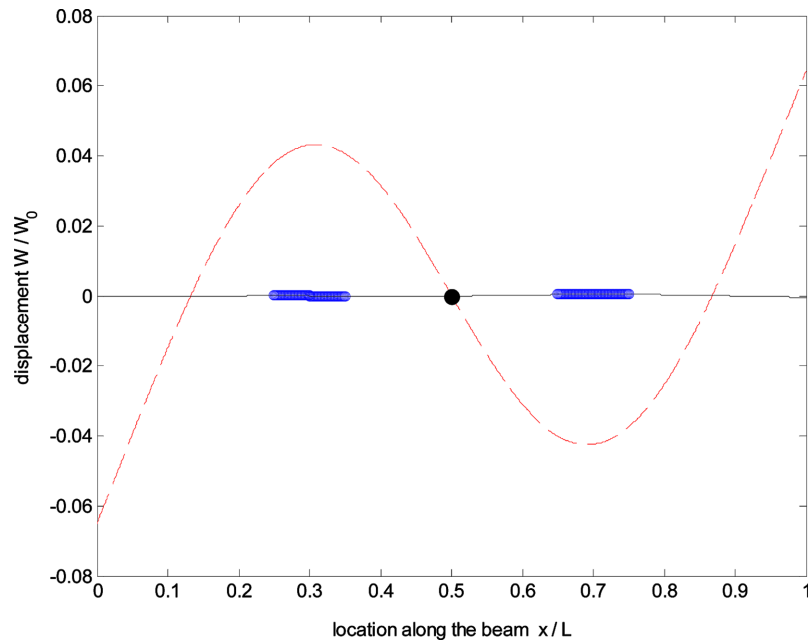


Fig. 8 The steady state deflection responses of loaded and unloaded panel when  $\hat{\omega} = 61.5$ ,  $\hat{x}_f = 0.45$ ,  $\hat{x}_m^1 = 0.3$ ,  $\hat{x}_m^2 = 0.7$ ,  $\hat{V}_0^1 = 0.0256 \times 10^{-6}$ ,  $\hat{V}_0^2 = -0.5144 \times 10^{-6}$ ; —, loaded; -----, bare; ●, mass  $M_s$

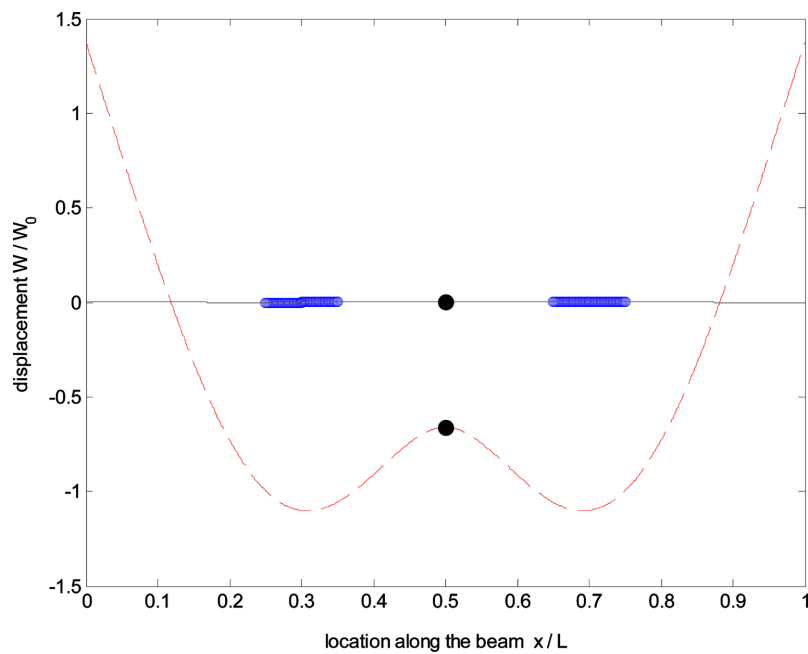


Fig. 9 The steady state deflection responses of loaded and unloaded panel when  $\hat{J}_s = 0.5$ ,  $\hat{\omega} = 70$ ,  $\hat{x}_m^1 = 0.3$ ,  $\hat{x}_m^2 = 0.7$ ,  $\hat{V}_0^1 = -0.00661 \times 10^{-5}$ ,  $\hat{V}_0^2 = 0.13836 \times 10^{-5}$ ; —, loaded; -----, bare; ●, mass  $M_s$

point of the second is at  $\hat{x}_m^2 = 0.7$ . The driving control voltages are found to be  $\hat{V}_0^1 = -0.0066 \times 10^{-5}$  and  $\hat{V}_0^2 = 0.13836 \times 10^{-5}$ .

## 6. Conclusions

The problem of achieving vibration suppression of composite satellite solar panel using piezoelectric patches that are driven by control voltages has been examined analytically. These patches are bonded by strong adhesive epoxy at arbitrary selected locations on the panel. The satellite panels are modeled as laminated composite beam using first-order shear deformation laminated plate theory which accounts for rotational inertia as well as shear deformation effects. The dynamic Green's function is utilized to provide a simple, exact and direct analytical method for analyzing the problem. Equally important, this procedure exhibits appreciably greater computational efficiency when compared with other approximate methods like finite element or modal superposition. In addition, any engineer can use it without any difficulty of a pragmatic nature.

## Acknowledgements

This work presented herein has been supported by the National Plan for Science and Technology (NPST-KSU); the Kingdom of Saudi Arabia under Grant number: 08-SPA237-2. These supports are greatly appreciated.

## References

- Abramovich, H. and Livshits, A. (1993), "Dynamic behavior of cross-ply laminated beams with piezoelectric layers", *Comp. Struct.*, **25**(1-4), 371-379.
- Abo-Hilal, M. (2003), "Forced vibration of Euler-Bernoulli beams by means of dynamic green function", *J. Sound Vib.*, **267**(2), 191-207.
- Bailey, T. and Hubbard, S.J. Jr. (1985), "Distributed piezoelectric polymer active vibration control of a cantilever beam", *J. Guid. Control. Dynam.*, **8**, 605-611.
- Banks, H.T., Smith, R.C. and Wang, Y. (1996), *Smart material structures: modeling, estimation and control*, Wiley, Paris, France.
- Bergman, L.A. and Hyatt, J.H. (2003), "Green functions for transversely vibrating uniform beam Euler-Bernoulli beams subject to constant axial preload", *J. Sound Vib.*, **134**, 175-180.
- Chen, C.Q. and Shen, Y.P. (1997), "Optimal control of active structures with piezoelectric modal sensors and actuators", *Smart Mater. Struct.*, **6**(4), 403-409.
- Foda, M.A., Almajid, A.A. and ElMadany, M.M. (2010), "Vibration suppression of composite laminated beams using distributed piezoelectric patches", *Smart Mat. Struct.*, **19**(11), 115018-115026.
- Foda, M.A. and Alsaif, K.A. (2009), "Control of lateral and angular vibrations at desired locations along vibrating beam", *J. Vib. control.*, **15**(11), 1649-1678.
- Garcia, E., Dosch, J. and Inman, D. (1992), "The application of smart structures to the vibration suppression problem", *J. Intel. Mater. Syst. Struct.*, **3**(4), 659-667.
- Gibbs, G.P. and Fuller, C.R. (1992), "Excitation of thin beams using asymmetric piezoelectric actuators", *J. Acoust. Soc. Am.*, **92**, 3221-3227.
- Hagood, N.W. and Chung, W.H. (1990), "Modeling of piezoelectric actuator dynamics for active structural control", *J. Intel. Mater. Sys. Struct.*, **1**, 327-354.

- Honda, S, kajiwara, I and Narita, Y. (2011), “Multidisciplinary design optimization for vibration control of smart laminated composite structures”, *J. Intel. Mater. Sys. Struct.*, **22**, 1419-1430.
- IEEE Standard on Piezoelectricity (1988), ANSI/IEEE Std. 176-1987, The Institute of Electrical and electronics Engineers, Inc. New York.
- Kayacik, Ö., Bruch. J.C. Jr, Sloss, J.M., Adali, S. and Sadek, I.S. (2008), “Integral approach for piezo patch vibration control of beams with various type of damping”, *Comput. Struct.*, **86**(3-5), 357-366.
- Kedziora, P. and Muc, A. (2012) “Optimal shapes of PZT actuators for laminated structures subjected to displacement or eigenfrequency constraints”, *Comput. Struct.* **94**, 1224-1235.
- Kim, Y., Suk, J.Y. and Junkins, J.L. (1995), “Optimal slewing and vibration control of smart structures”, *SPIE*, **2443**, 157-170.
- Jones, R.M. (1975), *Mechanic of Composite Materials*, McGraw, Hill, New York.
- Li, X.F. (2008), “A unified approach for analyzing static and dynamic behaviors of a functionally graded Timoshenko beam and Euler-Bernoulli beams”, *J. Sound Vib.*, **318**(4-5), 1210-1229.
- Lueg, P. (1936), *U.S Patent No. 2043416*, Process of silencing sound oscillations.
- Ma, K. and Ghasemi-Nejhad, M.N. (2004), “Frequency-weighted adaptive control for simultaneous precision positioning and vibration suppression of smart structures”, *J. Smart Mater. Struct.*, **13**(5), 1143-1154.
- Madabhushi-Raman, P. and Davalos, J.F. (1996), “Static shear correction factor for laminated rectangular beams”, *Compos. Part B - Eng.*, **27**(3-4), 285-293.
- Moulson, A.J. and Herbert, J.M. (1990), *Electroceramics: materials, properties, applications*, Chapman and Hall, London, U K.
- Olson, H.F. (1956), “Electronic control of mechanical noise, vibration reverberations”, *J. Acoust. Soc. Am.*, **28**, 966-972.
- Preumont, A. (2002), *Vibration control of active structures: an introduction*, 2<sup>nd</sup> Ed., Kluwer Academic, Dordrecht.
- Roach, G. (1981), *Greens functions*, Cambridge Univ. Press, Cambridge U K.
- Reddy, J.N. (1996), *Mechanics of laminated composites plates: theory and analysis*, CRC Press, New York.
- Srinivasan, A.V. and McFarland. D. (2001), *Smart structure analysis and design*, Cambridge Univ. Press, Cambridge, U.K.
- Tzou, H.S. (1993), *Piezoelectric shells-distributed sensing and control of continua*, Kluwer Academic, New York.
- Vinson, J.R. and Sierakowski, R.L. (1986), *The behavior of structures composed of composite materials*, Springer Verlag, Berlin.

CC

## Nomenclature

$b$	: panel width
$D_{11}^*$	: composite panel flexural stiffness
$E_{pe}$	: Young modulus of a piezoelectric patch
$f_{ext}(x,t)$	: excitation force per unit length
$F_0$	: excitation force amplitude
$G(x,u)$	: Green's function.
$G_u(x,u)$	: partial first derivative of the Green's function w.r.t $u$
$G_{xx}(x,u)$	: partial second derivative of the Green's function w.r.t $x$
$G_{uxx}(x,u)$	: partial derivative of the Green's function w.r.t $u$ and $x$
$H(\cdot)$	: Heviside step function
$h_a$	: height of the piezoelectric patch
$h_b$	: half height of the panel
$k'$	: shear factor
$K_s$	: composite panel shear rigidity

$I_0$	: mass of a composite panel per unit length
$I_2$	: mass moment of inertia of a composite panel
$J_s$	: mass moment of inertia of satellite body
$M_s$	: mass of satellite body
$m_{pe}^i$	: mass of the $i$ th piezoelectric patch per unit length
$q(x, t)$	: applied force per unit length of the panel
$t$	: time variable
$V_0$	: PZT patch actuating voltage
$w(x, t)$	: panel transverse deflection
$W(x)$	: panel spatial transverse deflection
$x$	: axial coordinate along the panel
$x_1^i$	: left edge coordinate of $i$ th piezoelectric patch
$x_2^i$	: right edge coordinate of $i$ th piezoelectric patch
$x_m^i$	: mid-point coordinate of $i$ th piezoelectric patch
$x_f$	: location of the localized excitation force
$\delta(\cdot)$	: Dirac delta function
$\delta'(\cdot)$	: first derivative of the Dirac delta function
$\rho$	: density of panel material
$\omega$	: excitation frequency

## Appendix

The displacement field is of the form

$$\begin{aligned} u &= u_0(x, y, t) + z\phi_x(x, y, t) \\ v &= v_0(x, y, t) + z\phi_y(x, y, t) \\ w &= w_0(x, y, t) \end{aligned} \quad (A1)$$

Where  $u_0, v_0, w_0$  are the mid-plane translational displacement components along the  $x, y, z$  coordinate directions; respectively, and  $\phi_x, \phi_y$  denote the rotations of a transverse normal about the  $y$  and  $x$  axes; respectively.

The strains associated with the above displacement field are given by

$$\begin{aligned} \varepsilon_x &= \frac{\partial u_0}{\partial x} + z\frac{\partial \phi_x}{\partial x}, & \gamma_{xy} &= \left(\frac{\partial u_0}{\partial y} + \frac{\partial v_0}{\partial x}\right) + z\left(\frac{\partial \phi_x}{\partial y} + \frac{\partial \phi_y}{\partial x}\right) \\ \varepsilon_y &= \frac{\partial v_0}{\partial x} + z\frac{\partial \phi_y}{\partial y}, & \gamma_{xz} &= \frac{\partial w_0}{\partial x} + \phi_x \\ \varepsilon_z &= 0, & \gamma_{yz} &= \frac{\partial w_0}{\partial y} + \phi_y \end{aligned} \quad (A2)$$

where  $z$  is the distance of the lamina from the mid-plane of the laminate.

In the usual notation, the stress strain relations in principle material coordinates for the  $k$ th lamina under plane stress are

$$\begin{Bmatrix} \sigma_1 \\ \sigma_2 \\ \sigma_{12} \end{Bmatrix}^{(k)} = \begin{bmatrix} Q_{11} & Q_{12} & 0 \\ Q_{12} & Q_{22} & 0 \\ 0 & 0 & Q_{66} \end{bmatrix}^{(k)} \begin{Bmatrix} \varepsilon_1 \\ \varepsilon_2 \\ \varepsilon_{12} \end{Bmatrix}^{(k)} \quad (A3)$$

where  $Q_{ij}$  ( $i, j = 1, 2, 6$ ) are the reduced stiffness which are defined in terms of engineering constants as

$$\begin{aligned} Q_{11} &= E_1/(1 - \nu_{12}\nu_{21}), & Q_{22} &= E_2/(1 - \nu_{12}\nu_{21}) \\ Q_{12} &= \nu_{12}E_2/(1 - \nu_{12}\nu_{21}), & Q_{66} &= G_{12} \end{aligned} \quad (A4)$$

Where  $E_1, E_2$  are the lamina longitudinal Young's modulus in directions 1 and 2 respectively while  $\nu_{12}$  is the Poisson ratio in plane 1-2 ( $\nu_{12}E_2 = \nu_{21}E_1$ ).

In the laminate coordinate systems ( $x, y, z$ ), the transformed stress are

$$\begin{Bmatrix} \sigma_x \\ \sigma_y \\ \sigma_{xy} \end{Bmatrix}^{(k)} = \begin{bmatrix} \bar{Q}_{11} & \bar{Q}_{12} & \bar{Q}_{16} \\ \bar{Q}_{12} & \bar{Q}_{22} & \bar{Q}_{26} \\ \bar{Q}_{16} & \bar{Q}_{26} & \bar{Q}_{66} \end{bmatrix}^{(k)} \begin{Bmatrix} \varepsilon_x \\ \varepsilon_y \\ \varepsilon_{xy} \end{Bmatrix}^{(k)} \quad (A5)$$

where the transformed stress  $\overline{Q}_{ij}$  are given in terms of the reduced stiffness  $Q_{ij}$  through the transformation equations which take into account the orientation of the laminae (Reddy 1996).

Substituting the strain displacement relation given by Eq. (A2) into Eq. (A5) and integrating through the height of the laminate, the following constitutive equations for symmetric laminate in the absence of in-plane forces is written as

$$\begin{Bmatrix} M_x \\ M_y \\ M_{xy} \end{Bmatrix} = \begin{bmatrix} D_{11} & D_{12} & D_{16} \\ D_{12} & D_{22} & D_{26} \\ D_{16} & D_{26} & D_{66} \end{bmatrix} \begin{Bmatrix} \frac{\partial \phi_x}{\partial x} \\ \frac{\partial \phi_y}{\partial y} \\ \frac{\partial \phi_x}{\partial y} + \frac{\partial \phi_y}{\partial x} \end{Bmatrix} \quad (\text{A6})$$

$$\begin{Bmatrix} Q_y \\ Q_x \end{Bmatrix} = k' \begin{bmatrix} A_{44} & A_{45} \\ A_{45} & A_{55} \end{bmatrix} \begin{Bmatrix} \frac{\partial w}{\partial y} + \phi_y \\ \frac{\partial w}{\partial x} + \phi_x \end{Bmatrix} \quad (\text{A7})$$

Where

$$D_{ij} = \frac{1}{3} b \sum_{k=1}^N \overline{Q}_{ij} (z_{k+1}^3 - z_k^3), \quad i, j = 1, 2, 6$$

$$A_{ij} = b \sum_{k=1}^N \overline{Q}_{ij} (z_{k+1} - z_k), \quad i, j = 4, 5 \quad (\text{A8})$$